

# On Continuous Phase Modulation in Cellular Digital Mobile Radio Systems

By C.-E. SUNDBERG\*

(Manuscript received January 19, 1982)

This paper considers the application of constant-amplitude, partial-response, continuous-phase modulation with simple near-optimum receivers to cellular digital mobile radio systems. These smoothed modulation schemes have low spectral sidelobes and narrow main lobes. A combiner for time-division retransmission systems with space diversity is given for continuous-phase modulation. Cochannel interference and adjacent-channel interference are calculated for continuous-phase modulation in cellular systems with frequency reuse. The efficiency of 3RC and 4RC modulations with space diversity is evaluated for conventional cellular systems.

## I. INTRODUCTION

This paper considers a class of constant-amplitude digital modulation schemes with smoothed partial-response, continuous-phase modulation. This gives a bandwidth-efficient digital modulation scheme. With the baseband quadrature combiner described below, these modulation schemes can also be used with time-division retransmission. The concept of time-division retransmission is briefly described below. This scheme makes it possible to use simple equipment at the mobile unit, and yet use several branches of space diversity, assuring a reasonable error rate on the fading channel. Most of the signal processing and all diversity combining is performed at the base stations.

To obtain good spectral efficiency in digital mobile radio systems,

---

\* Bell Laboratories. Currently at the University of Lund, Sweden.

---

©Copyright 1983, American Telephone & Telegraph Company. Photo reproduction for noncommercial use is permitted without payment of royalty provided that each reproduction is done without alteration and that the Journal reference and copyright notice are included on the first page. The title and abstract, but no other portions, of this paper may be copied or distributed royalty free by computer-based and other information-service systems without further permission. Permission to reproduce or republish any other portion of this paper must be obtained from the Editor.

frequency reuse is employed.<sup>1-4</sup> Each cell in the cellular system is assigned a number of channels in a frequency division system. Each channel (frequency) is reused at a cell further away. The closer this cell is, the larger the number of available channels. On the other hand, the signal-to-cochannel interference increases when the interfering cells are too close. The interference is also affected by the way the base-station antennas are arranged. Omnidirectional and directional antennas have been considered. Furthermore, the location of the base station in the cell is important for the signal-to-interference ratio. In this paper we consider two schemes: Centrally located base stations with omnidirectional antennas, and cooperating base stations with 120-degree directional antennas in three alternate corners in a hexagonal cell. Below, we will see how cochannel and adjacent-channel interference is calculated for continuous-phase modulation in a cellular environment.

The rest of this paper is organized as follows. Section II contains background material on modulation methods, conventional cellular systems, time-division retransmission, and propagation and interference models used in the analysis. Section III presents a baseband maximal-ratio combiner for time-division retransmission with constant-amplitude modulations. Section 4.1 contains the calculations of signal-to-cochannel interference ratios for cellular systems with continuous-phase modulation. Section 4.2 gives some results on adjacent-channel interference. Section V contains a discussion and conclusions.

## II. BACKGROUND MATERIAL

Before the cellular systems are discussed in any detail, we will give some brief background information about the class of constant-amplitude modulation systems considered in this paper, conventional cellular arrangement, the time-division retransmission method, and signal propagation and interference models for the fading land mobile radio channel.

### 2.1 Constant-amplitude modulations

Constant-amplitude modulation schemes are considered for application to cellular digital mobile radio systems. The transmitted signal is of the form

$$s(t) = \sqrt{\frac{2E}{T}} \cos[\omega_c t + \phi(t)], \quad (1)$$

where the information-carrying phase is

$$\phi(t) = 2\pi h \sum_i \alpha_i q(t - iT), \quad (2)$$

with

$$q(t) = \int_0^t g(\tau) d\tau. \quad (3)$$

The pulse shape  $g(t)$  (instantaneous frequency) determines the spectral behavior of the modulation scheme, while  $h$  is the modulation index, and the  $\alpha_i$ 's are data symbols. For detailed background on these schemes, see Refs. 5-11. In this paper, we will mainly concern ourselves with schemes having modulation index  $h = 1/2$  and with  $g(t)$  in the form of raised cosine pulses of length  $LT$ , where  $T$  is the bit time. This pulse shape is defined by

$$g(t) = \begin{cases} \frac{1}{2LT} \left[ 1 - \cos \left( \frac{2\pi t}{T} \right) \right] & 0 \leq t \leq LT \\ 0 & t \leq 0, t \geq LT. \end{cases} \quad (4)$$

For  $L > 1$ , the pulses are overlapping in time, thus creating controlled intersymbol interference. In this paper, only binary transmission  $\alpha_i = \pm 1$  will be considered. The reason is that binary schemes with modulation index  $h = 1/2$  have simple, near-optimum receivers, i.e., "minimum shift keying (MSK)-type" receivers (see Refs. 7-9).

Figures 1 to 3 show examples of power spectra of (unfiltered)

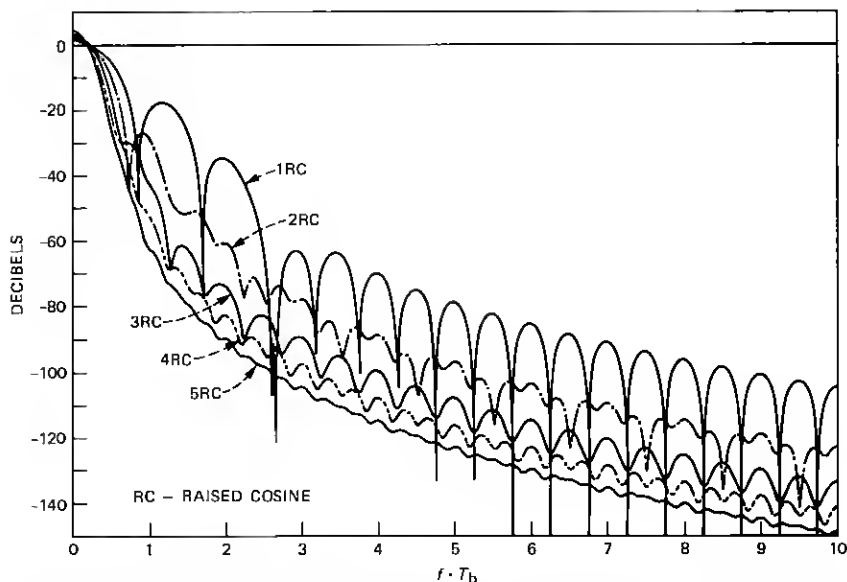


Fig. 1—Power spectra for binary RC schemes when  $h = 1/2$ ,  $L = 1$  to 5. For details, see Refs. 5, 6, and 11.  $T_b$  is bit time (symbol time). (Spectra are shown one-sided normalized with total power.)

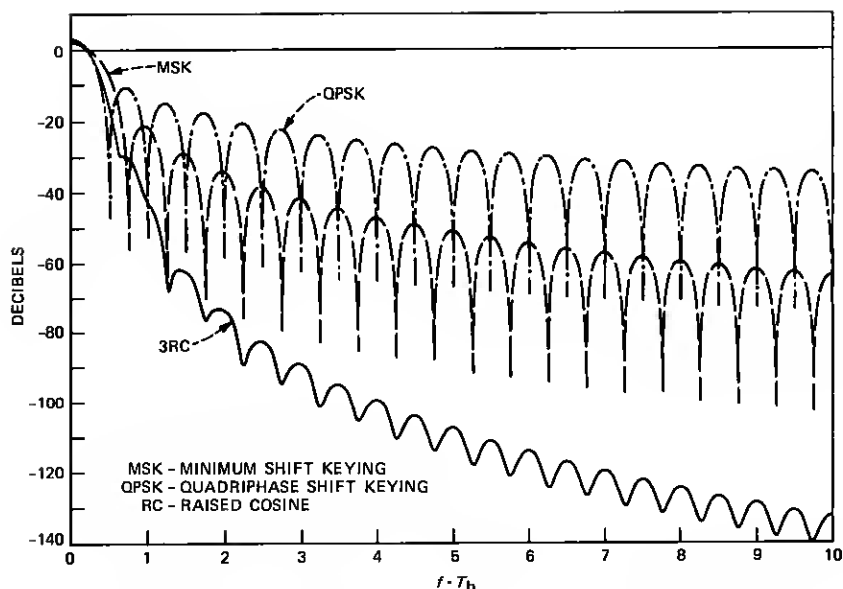


Fig. 2—Power spectra for binary 3RC with  $h = 1/2$ , QPSK, and MSK.

constant-amplitude modulation schemes in the raised cosine family. A scheme with a pulse shape  $g(t)$  of a raised cosine shape with length  $3T$  is denoted by 3RC (raised cosine). Minimum shift keying,<sup>9</sup> tamed frequency modulation (TFM),<sup>8</sup> and Gaussian MSK (GMSK)<sup>10</sup> are obtained from eqs. (1) and (2) by selecting proper pulses  $g(t)$  (see Refs. 5 to 7 for details).

Even better spectral tail behavior is obtained with spectral raised cosine (SRC) pulse shapes instead of raised cosine pulse shapes.<sup>5,6</sup> These schemes are more difficult to analyze exactly, however. A 3SRC pulse  $g(t)$  has a length of  $3T$  between the first nulls in time around the peak value. The Fourier Transform is a raised cosine. Thus, the time function is infinitely long. In practice, these pulses are truncated.

Figures 4 and 5 show examples of error probability curves for coherent binary phase shift keying (BPSK), quadriphase shift keying (QPSK), 3RC and 4RC for slow Rayleigh fading, space diversity with  $M$  branches, and ideal maximal-ratio combining. These are examples of calculations in Refs. 7 and 12. The analysis for the Gaussian channel is presented in Ref. 7, using analytical tools from Refs. 13 and 14. The formulas for the Gaussian channel are generalized to the fading channel in Ref. 12. Note that the error probability curves in Figs. 4 and 5 are shown without differential encoding/decoding. In practice, differential encoding is employed as the simplest way of resolving phase ambiguity in the coherent MSK-type receiver for  $h = 1/2$

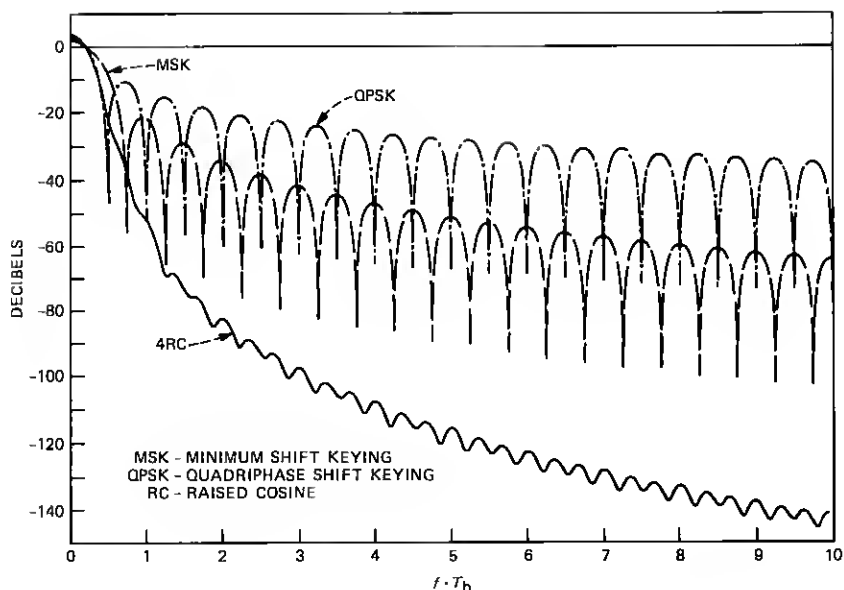


Fig. 3—Power spectra for binary 4RC with  $h = 1/2$ , QPSK, and MSK.

schemes.<sup>7,8,9,15</sup> For this case, all error probability values in Figs. 4 and 5 are multiplied by a factor of two.

The longer the pulse  $g(t)$ , the more narrow the power spectrum.<sup>6</sup> However, the detection efficiency is reduced with increasing  $L$  for fixed  $h = 1/2$ , particularly for suboptimum receivers.<sup>7</sup> The optimum receiver (the Viterbi detector) is more robust.<sup>6</sup> Thus, as we will see, choosing the length of the pulse shape  $g(t)$  plays an important part in the overall system optimization.

Power amplifiers, both in the mobile unit and at the base stations, sometimes contain nonlinearities. For such cases, it is advantageous to use a constant envelope modulation scheme. Such a scheme will not be subject to widened spectra after the nonlinearity. This is the case for nonconstant amplitude modulations. A QPSK signal passed through a bandpass filter can be quite narrowband. The signal amplitude varies, however, and after a nonlinearity, the sidelobes are restored to a level that is unacceptable from an adjacent-channel interference point of view.

## 2.2 Conventional cellular arrangement

This paper will consider frequency reuse in cellular systems for digital mobile radio systems. Figure 6a shows an example of a cellular system with  $N = 3$  hexagonal cells per cluster. Frequencies are assigned as in Fig. 6b. Note that for a fixed total number of channels, a fixed

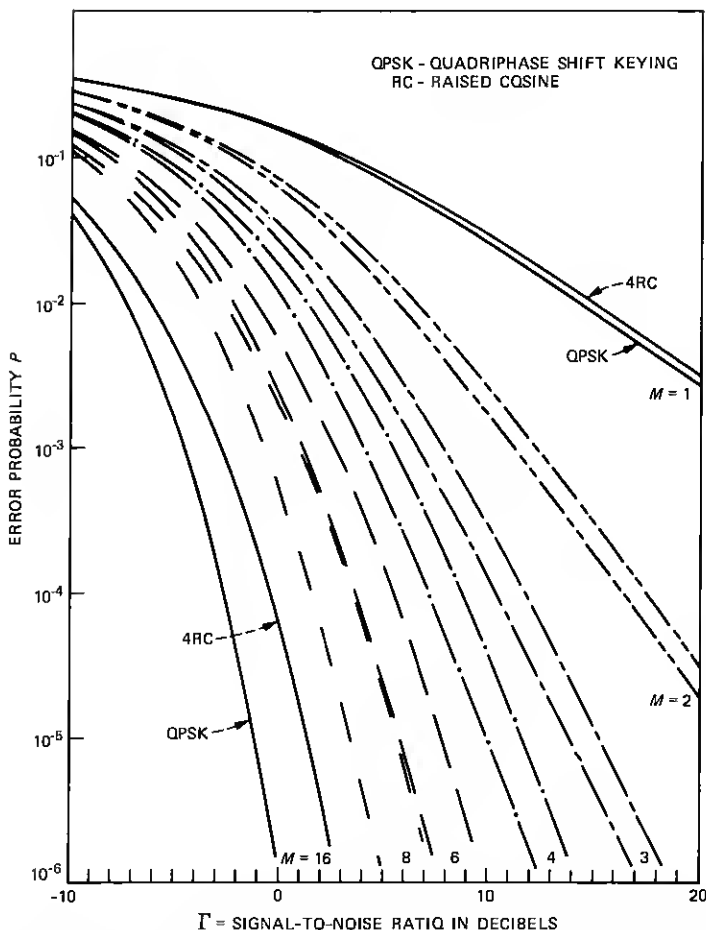


Fig. 4—Error probability,  $P$ , versus average per diversity branch (and per bit) signal-to-noise ratio  $\Gamma$  for a coherent MSK-type receiver with Selected Pulse Amplitude Modulation (SPAM) receiver. Maximal-ratio combining and modulation scheme 4RC are used. Curves shown without differential encoding/decoding.

antenna configuration, and a fixed cell size, a large frequency reuse factor,  $N$ , gives good cochannel interference (the interfering cells get further away) but low system capacity, since the number of available channels in one cell is inversely proportional to  $N$ .<sup>1-3</sup> In this paper, we will basically confine the discussion to one type of cell, namely the type with three 120-degree corner antennas, as shown in Fig. 7. The maximum distance from any base station  $d_0$  is equal to the cell radius  $r$ . For details about cellular systems based on this cell, see Refs. 1 and 3. Other cellular concepts are considered in Ref. 16.

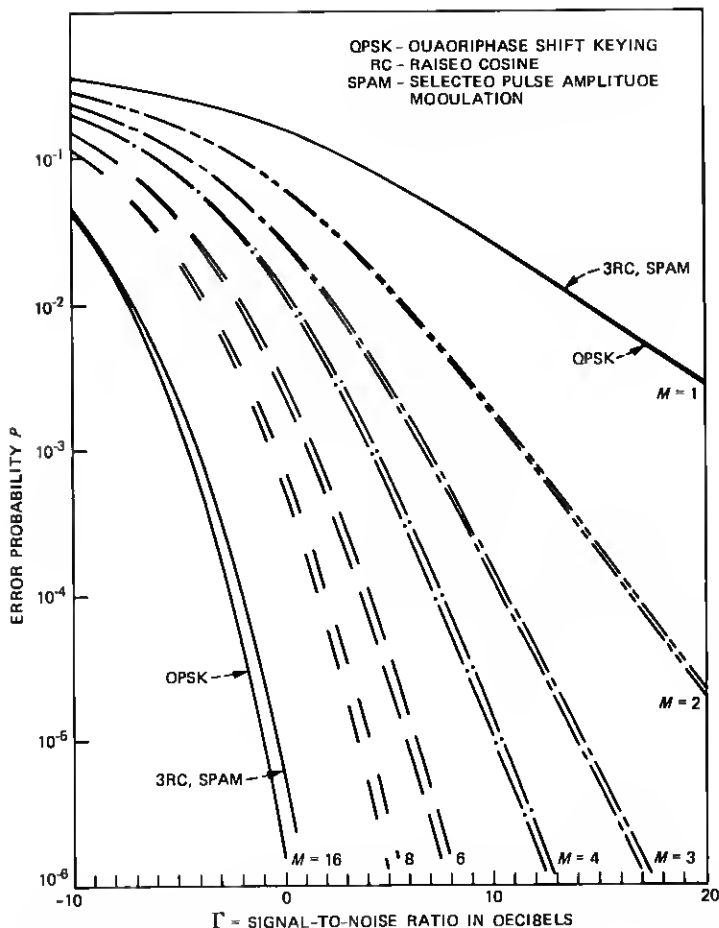


Fig. 5—Same as Fig. 4 with 3RC and SPAM-filter  $M$  branch diversity with maximal-ratio combining.

### 2.3 Time-division retransmission

The time-division retransmission (TDR) concept is described in Refs. 3 and 4. The basic ideas are as follows. The fading channel changes "slowly" (during one burst or package). Communication in both directions takes place in packages transmitted in the same frequency band: first mobile-to-base and then base-to-mobile. During mobile-to-base transmission, the channel is estimated for maximal-ratio, space-diversity combining in both directions. Several schemes<sup>3</sup> have been proposed for performing the required co-phasing for transmission from and reception at the base station. Because all diversity combining takes place at the base stations, the mobile equipment is

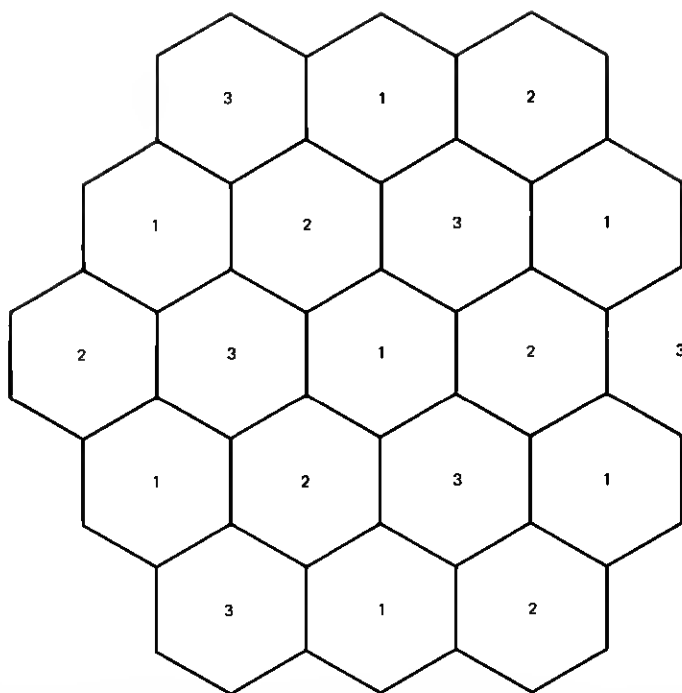


Fig. 6a—Example of cellular system. Each cell is a hexagon of equal area, and frequencies are reused. Cells marked with same digit use same frequency channel set (see Fig. 6b). In cluster of  $N = 3$  cells, all channels are used.

relatively simple. As a consequence, it is feasible to use more than two branches of diversity with TDR.

## 2.4 Signal propagation and interference

It is assumed that mobile radio reception in an urban environment is characterized by

$$P(\vec{r}) = |\vec{r}|^{-\alpha} S(\vec{r}) \cdot R^2(\vec{r}), \quad (5)$$

where  $P(\vec{r})$  is the received signal power at location  $\vec{r}$  (position vector relative to a transmitter).<sup>1,3,4</sup> The first factor,  $|\vec{r}|^{-\alpha}$ , is a reduction factor due to the distance between the mobile unit and the transmitter, and  $\alpha$  is the propagation constant. It is normally assumed that  $\alpha$  is in the range three to four in the urban environment.<sup>1,3</sup> In free space,  $\alpha = 2$ .

The second factor,  $S(\vec{r})$ , represents shadow fading,<sup>1,3,4</sup> and the third factor,  $R^2(\vec{r})$ , represents Rayleigh fading.<sup>4,17</sup>  $R$  is the envelope of the received signal and is modeled as a random variable with the density function



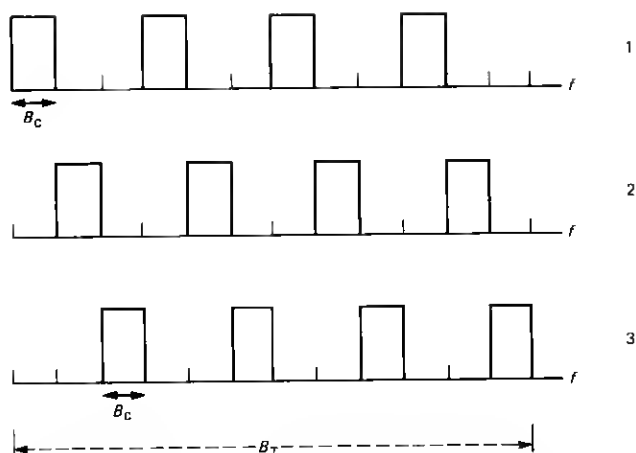


Fig. 6b—Frequency plan for cellular system with  $N = 3$ , shown in Fig. 6a. Channel set marked 1 used in each cell marked 1, etc. Channel bandwidth is denoted  $B_c$ , and total system bandwidth is  $B_T$ . Channel means two-way channels, including overhead for synchronization (when required).

$$p(R) = 2Re^{-R^2}, \quad (6)$$

with  $E\{R^2\} = 1$  (see Refs. 4 and 17). In general,  $R$  varies with vehicle location and signal frequency.

This paper also considers propagation and interference in cellular systems with frequency reuse. We will make use of the same basic assumptions as in Refs. 1 and 3.

It is assumed that the cochannel interference and adjacent-channel interference from cells other than those containing the desired mobile unit are formed by the incoherent sum of contributions from many interfering sources. This sum is assumed to be equivalent to stationary Gaussian noise.<sup>1,3</sup> It is also assumed that the shadow and Rayleigh fading of the total interference is negligible compared to the fading of the signal.<sup>1,3,4</sup>

It is also assumed that cochannel interference is the main source of additive signal degradation. Adjacent-channel interference from other cells will be considered to some extent in a few cases, where it is assumed that the adjacent-channel interference is the incoherent sum of many sources forming a stationary additive Gaussian adjacent-channel noise, which is added to the cochannel interference. The additive thermal background noise is assumed to be negligible compared to the cochannel and the adjacent-channel interference. Thus, the transmitter power and the cell sizes are assumed to be such that alien background noise from sources other than mobile units and transmitters in the cellular system is negligible compared to cochannel and adjacent-channel interference.

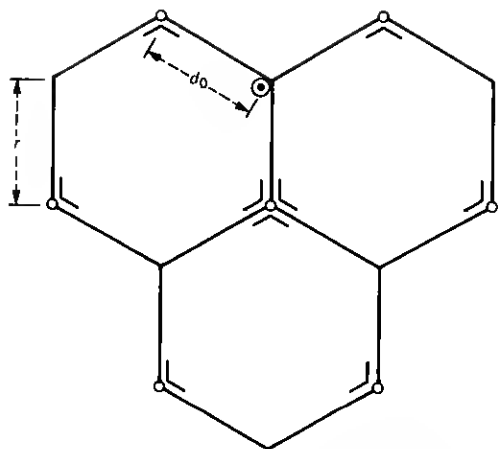


Fig. 7—Details for conventional three-corner, 120-degree antenna cell. Desired mobile shown in its worst-case locations.

Below, we will use the same technique as in Refs. 1 and 3 for calculating adjacent-channel interference and cochannel interference for continuous-phase modulation schemes. The signal-to-interference ratio is defined as the ratio of the signal power to the total noise power, based on the  $|F|^{-\alpha}$  propagation law and averaged over shadow and Rayleigh fading. It is assumed that the fading is flat over the band of each channel.

### III. A BASEBAND COMBINER FOR TIME-DIVISION RETRANSMISSION WITH CONSTANT-AMPLITUDE MODULATION

The time-division retransmission (TDR) concept has so far been applied only to binary modulation schemes with nonconstant amplitude.<sup>3</sup> For constant-amplitude modulation schemes, such as continuous-phase modulation, the combiner in Ref. 3 needs to be slightly generalized. That is the subject of this section. We have not yet analyzed the impact of the constant-amplitude format on synchronization. As a first rough estimate, it is assumed that the same scheme as that in Ref. 3 can be used also for constant-amplitude modulation. Further work in considering other schemes<sup>3</sup> for synchronization and establishing phase references is required for constant-amplitude modulation schemes.

The baseband combiner for space diversity with maximal-ratio combining used by P. S. Henry and B. Glance<sup>3</sup> for binary phase shift keying (BPSK) is easily generalizable to quadrature constant-amplitude modulation. The base-station signal processing equipment for one branch of diversity is shown in Fig. 8 for time-division retransmission with quadrature constant-amplitude modulation. During the

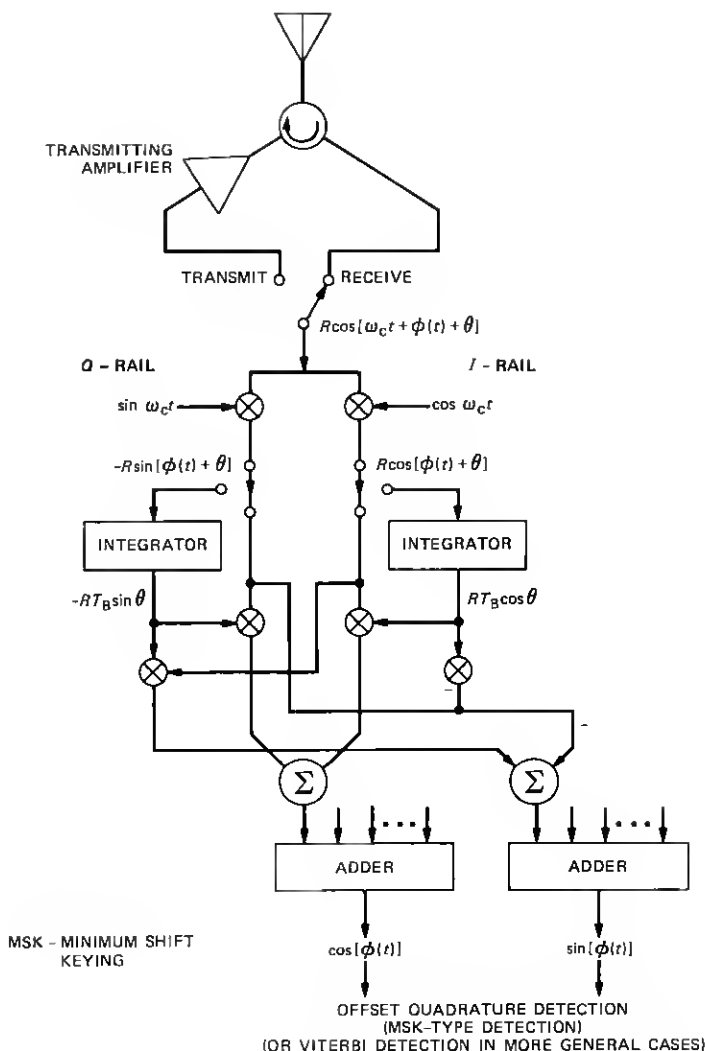


Fig. 8—Baseband combiner for constant-amplitude modulation and time-division retransmission. Compare this to Fig. 5 in Ref. 3.

reference transmission interval, the carrier burst of duration  $T_B$  is received, having the form

$$R \cos(\omega_c t + \theta), \quad (7)$$

where  $R$  is the Rayleigh amplitude, and  $\theta$  is the unknown phase. It is assumed that the  $R$  and  $\theta$  are essentially constant until the next reference burst is transmitted.<sup>3</sup> Then the stored  $R$  and  $\theta$  are updated.

After down-conversion and integration, the reference coefficients  $T_B R \cos \theta$  and  $T_B R \sin \theta$  are produced and stored for message demodulation. During information transmission, the received signal can be written

$$R \cos[\omega_c t + \phi(t) + \theta] + I_c \cos \omega_c t + I_s \sin \omega_c t, \quad (8)$$

where  $\phi(t)$  is the information-carrying phase (see the introduction).  $I_c$  and  $I_s$  are Gaussian interference with zero mean and variance  $S^2$  (see Ref. 3). After down-conversion and multiplication with the reference coefficients and combinations following the network in Fig. 8, we have in each quadrature arm the signals

$$\begin{aligned} S_I &= T_B R^2 \cos [\phi(t) + \theta] \cdot \cos \theta \\ &+ T_B R^2 \sin [\phi(t) + \theta] \cdot \sin \theta \\ &+ I_c T_B R \cos \theta - I_s T_B R \sin \theta \end{aligned} \quad (9)$$

in the cosine branch (*I*-rail), and

$$\begin{aligned} S_Q &= T_B R^2 \sin [(\phi(t) + \theta)] \cdot \cos \theta \\ &- T_B R^2 \cos [\phi(t) + \theta] \cdot \sin \theta \\ &- I_c T_B R \sin \theta + I_s T_B R \cos \theta \end{aligned} \quad (10)$$

in the sine branch (*Q*-rail). Using simple trigonometric formulas we have

$$S_I = T_B R^2 \cos[\phi(t)] + I_c T_B R \cos \theta - I_s T_B R \sin \theta, \quad (11)$$

$$S_Q = T_B R^2 \sin[\phi(t)] - I_c T_B R \sin \theta + I_s T_B R \cos \theta. \quad (12)$$

The special case of BPSK in Ref. 3 is obtained by letting  $\phi(t)$  be

$$\phi(t) = \begin{cases} 0 & \text{for data } +1 \\ \pi & \text{for data } -1. \end{cases} \quad (13)$$

Thus  $\cos \phi(t) = \pm 1$ , and  $\sin \phi(t) = 0$ . Only one output is required in this case. Maximal-ratio combining at the output is obtained by adding the components from the  $M$  branches.<sup>3</sup> Coherent reception is obtained and the data can be demodulated by processing  $\cos \phi(t)$  and  $\sin \phi(t)$ . This can, for example, be done by means of the "MSK-type" receiver (offset quadrature receiver)<sup>7-9</sup> or, for the more general case, even a Viterbi detector.<sup>6,13</sup>

The combiner in Fig. 8 followed by an "MSK-type receiver" supplies the motivation for considering the family of  $h = 1/2$  partial response FM or continuous-phase modulation (CPM) schemes<sup>6,7</sup> for the case of slow Rayleigh fading with  $M$ -branch space diversity with maximal-ratio combining.<sup>4,7</sup>

For transmission from the base station to the mobile unit, all stored phase references in Fig. 8 are changed from  $\theta$  to  $-\theta$ . Thus, through the time-division retransmission procedure, maximal-ratio combining is approximately obtained at the mobile unit with only one antenna and one receiver.<sup>3</sup> All signal processing is performed at the base-station transmitter.

#### IV. COCHANNEL AND ADJACENT-CHANNEL INTERFERENCE ANALYSIS FOR CPM

##### 4.1 *Cochannel interference analysis*

The technique for the cochannel interference analysis of CPM is basically the same as that for BPSK QPSK in Refs. 1, 3, and 16. The signal-to-cochannel interference ratios are given by the geometry of the cells and antennas and of the propagation exponent  $\alpha$  [in the range three (pessimistic) to four]. From Refs. 1 and 3, we have the average signal-to-cochannel interference ratio with a three-corner cell system with three cells per cluster

$$P_s/P_1 = 7.5 \text{ dB} \quad (14)$$

for mobile-to-base transmission and

$$P_s/P_1 = 8.0 \text{ dB} \quad (15)$$

for base-to-mobile transmission. Figure 4 shows the theoretical number of diversity branches required in a space diversity (TDR) 4RC and QPSK scheme. Figure 5 shows the corresponding curves for 3RC.

With a larger number of cells per cluster (large channel sets), the required signal-to-cochannel interference ratio is larger, and thus fewer diversity branches are required.

It is assumed in the calculations that the background noise from other sources is negligible. The calculated signal-to-interference ratio determines which modulation method can be used (in terms of required detection efficiency) and how many branches of diversity are required.

Note that the signal-to-cochannel interference ratio is not dependent on a particular modulation scheme. It is given by the relationships of distances from the desired base station to the desired mobile unit and from the interfering base stations or mobile units. See Refs. 1, 3, and 16 for details. Thus, the cell geometry gives the available signal-to-cochannel interference ratio. This number plus the bit error probability requirement determines the number of diversity branches for a given modulation scheme by using results like those in Ref. 12 (see Figs. 4 and 5).

Reference 16 gives cochannel interference results for a generalized class of cells.

## 4.2 Adjacent-channel interference analysis

The effect of adjacent-channel interference in cellular mobile radio systems is briefly considered for some cases with constant-amplitude modulation schemes.

Figure 9 shows the so-called fractional out-of-band power curves for the binary-raised cosine family for modulation index  $h = 1/2$ .<sup>6,7</sup> These curves show the fraction of the spectral power relative to the total power outside the band  $-f + f_0$ ,  $f + f_0$  for the data rate  $f_b = 1/T_b$ . Thus, the bandwidth of the 4RC with the portion  $10^{-3}$  of the total power outside the band is approximately  $0.95/T_b$ . Note that the figure shows half the bandwidth of one channel. Figures 10 and 11 show 3SRC and 4SRC. Similar curves for GMSK are published in Ref. 10.

Curves like those in Fig. 9 are useful for calculating the adjacent-

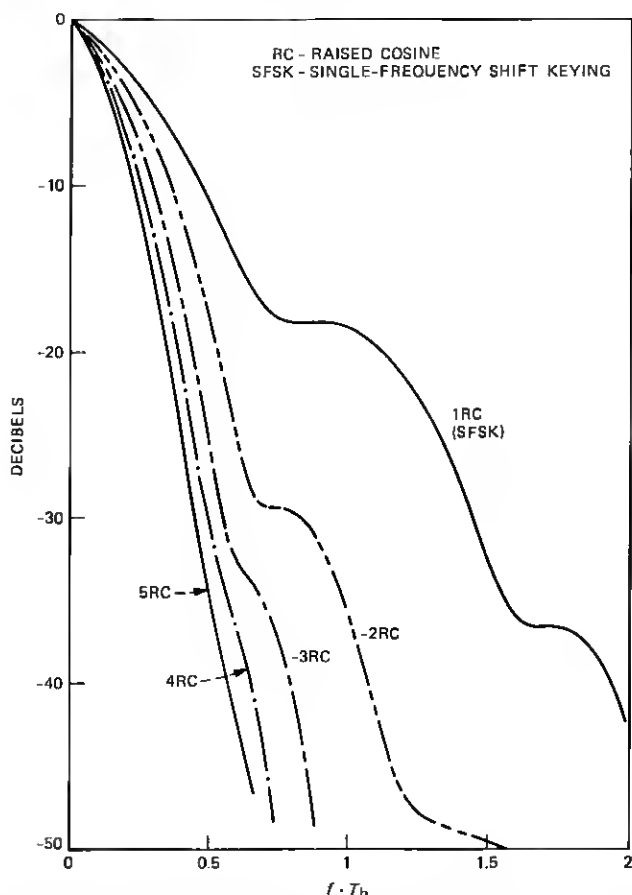


Fig. 9—Fractional out-of-band power curves for the binary modulation schemes 1RC, 2RC, 3RC, 4RC, and 5RC,  $h = 1/2$ .

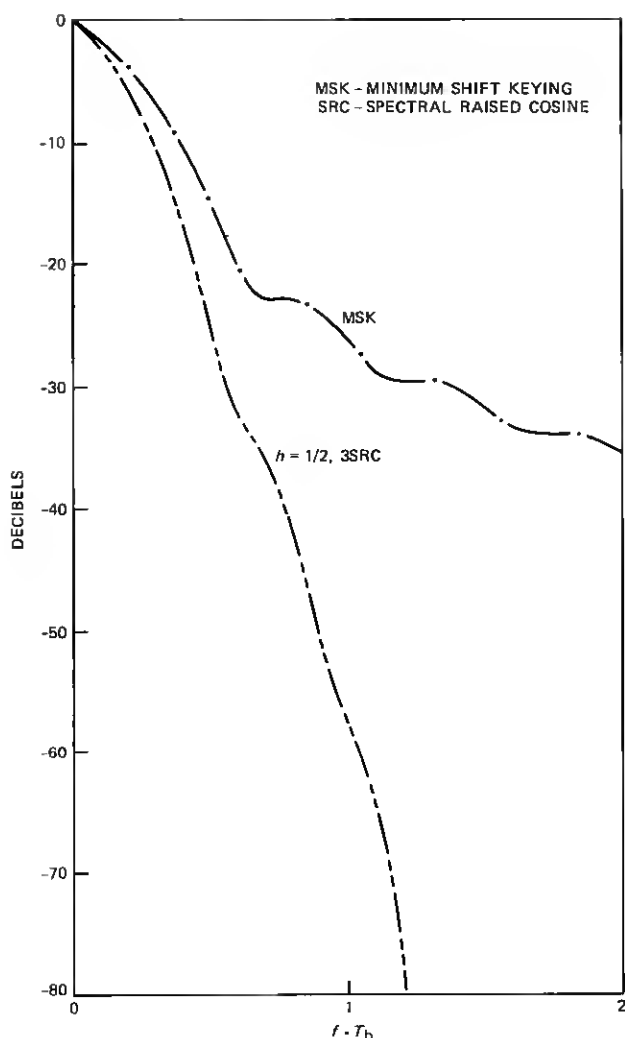


Fig. 10--Fractional out-of-band power curves for 3SRC,  $h = 1/2$ , and MSK.

channel interference. From the curves in Fig. 9, we obtain an upper bound on the interference power in the two adjacent channels on each side. Since the power spectra fall off rapidly with  $f$  for increasing frequencies, this upper bound is a good estimate of the adjacent-channel interference power level.

From the results in the appendix and from the cochannel interference results above and in Refs. 1, 3, and 16, it is evident that with "wide" channels compared to the bit rate, average adjacent-channel interference is very small compared to cochannel interference. In the

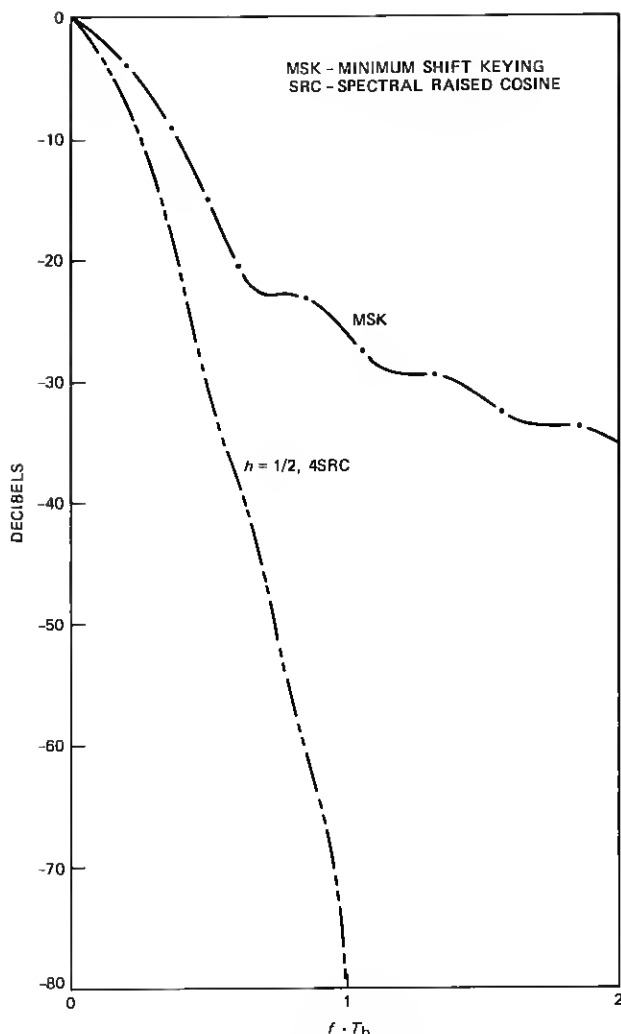


Fig. 11—Fractional out-of-band power curves for 4SRC,  $h = 1/2$ , and MSK.

appendix, a parameter,  $A$ , is introduced, which is a measure of the adjacent-channel interference suppression with a given modulation scheme and a given relationship between the bit rate and the channel bandwidth. Even with  $A$  as large as  $10^{-2}$ , the average adjacent-channel interference is almost negligible compared to the cochannel interference. Much smaller  $A$ 's are quoted in the literature ( $10^{-6}$ – $10^{-7}$ ).<sup>8,10,18</sup> With  $A$  as small as  $10^{-2}$ , the detection efficiency of the modulated signal will be affected by the filtering. In the system discussion below, we will choose "small"  $A$ 's.



For schemes with  $N \geq 3$ , the adjacent-channel interference with one particular cell is small with modulation schemes like 3RC-4RC (see Figs. 1, 6, and 7). The average adjacent-channel interference from adjacent cells is small compared to the cochannel interference. The same is true for  $N = 1$  for the adjacent-channel interference from adjacent cells. However, for  $N = 1$ , the adjacent-channel interference within one cell is a more severe problem. This will restrain the value of bit rate  $f_b$ , relative to the channel bandwidth  $B_c$ . Cellular systems with  $N = 1$  are considered in Refs. 1 and 16.

## V. DISCUSSION AND CONCLUSIONS

We can now put the various pieces of information together and evaluate the number of available channels for cellular schemes with different modulation schemes. Time-division retransmission is used in several cases but not all. For the cases without time-division retransmission, it is expected that the number of space diversity branches cannot be larger than  $M = 2$ . It is inconvenient to have more than two antennas on the mobile unit.

Let  $B_T$  be the total system bandwidth, and let  $B_c$  be the bandwidth of one two-way TDR channel (or two one-way channels without TDR). Let the bit rate over one channel be  $f_b = 1/T_b$  bits/s. The total number of available channels is  $B_T/B_c$ . Let  $N$  be the number of cells in a cluster. The number of channels,  $C$ , available in each cell in the cluster is  $B_T/B_c \cdot 1/N$ . The total system bandwidth will be kept constant for comparison of various systems. It is evident that  $C$  can be improved by decreasing  $N$  or decreasing  $B_c$  (at a given  $B_T$  and a given transmitted bit rate  $f_b$ ). Decreasing  $N$  has been discussed in Ref. 16. Decreasing  $B_c$  can be done to a certain degree by selecting narrowband modulation schemes. However, the detection efficiency decreases for schemes with simple receivers. Furthermore, the adjacent-channel interference increases. There seems to be a preferred modulation scheme with an intermediate degree of smoothing (see Ref. 7 for details). These we have chosen below.

The total system bandwidth is assumed to be 40 MHz, and the carrier frequency  $f_c = 850$  MHz. The propagation constant is  $\alpha = 3$ , and the error probability is  $10^{-3}$ . It is assumed that digitized speech is transmitted with 32 kb/s. If 16 kb/s is used (and all other system parameters are kept unchanged), the total system capacity in terms of channels is of course doubled for all schemes. When comparisons are made to other schemes,<sup>3,15</sup> these will be scaled to "our" system bandwidth 40 MHz and data rate  $f_b = 32$  kb/s.

The calculations of number of diversity branches given below assume ideal conditions all the way through, i.e., no degradation due to

filtering, nonlinearities, timing, synchronization, combining, etc. Sometimes there is a margin, though.

Below we will calculate the number of channels per cell (antenna) for a few different cases.

1.  $N = 3$ , i.e., a cell with 120-degree base stations in three corners. Time-division retransmission. BPSK with 81 kb/s data rate (the overhead over 64 kb/s is due to the co-phasing procedure for the TDR scheme). Channel bandwidth  $B_c = 100$  kHz (see Ref. 3). With this channel bandwidth, the transmitted BPSK signal must be filtered quite hard, resulting in a nonconstant amplitude.  $M = 3$  branch diversity. This scheme gives about 133 two-way channels.

2.  $N = 3$  and the same cells as in 1. TDR with 81 kb/s in a channel bandwidth of 81 kHz, 4RC (or better 4SRC<sup>6</sup>) modulation (see Figs. 9 to 11 for adjacent-channel interference estimates). Mild filtering of the 4RC might be necessary, causing small fluctuations of the envelope (see Fig. 4 for error probability considerations). TDR and  $M = 4$  branches of diversity. The number of channels is 164.

3.  $N \cong 11$ , a cell with centrally located, omnidirectional antenna.  $M = 2$  branches of diversity, no TDR. GMSK modulation with  $B_b T \cong 0.25$  (see Refs. 10 and 15 for parameter definitions and other details). This corresponds roughly to 3RC (3SRC). Adjacent-channel interference is about -70 dB. 64 kb/s in 107 kHz. The results in Ref. 15 were scaled to the total bandwidth of 40 MHz and the data rate of 32 kb/s in the one-way speech channel. About 33 channels are available.

4. Same as 3 above with harder filtering. 64 kb/s in 58 kHz. Adjacent-channel interference is about -20 dB.<sup>15</sup> This leads to 62 channels.

The reasons that schemes 3 and 4 above yield such a low number of channels compared to the others are twofold. Time-division retransmission is not considered. Therefore an  $M = 2$  is the highest degree of diversity considered. This leads to the high  $N$  value. The other important reason is that only centrally located omnidirectional antennas are considered. Thus, even with a good modulation scheme, the number of channels remains low.

A class of constant-amplitude modulation schemes is considered for the cellular digital radio system. Such features as power spectral density, fractional out-of-band power, and detection efficiency with simple near-optimum detectors for the slow Rayleigh fading channel with space diversity and maximal-ratio combining are reported.

From the analysis and discussions above, we have seen that a large number of channels can be provided in a digital cellular system by the proper combination of antenna configuration, modulation scheme, and diversity scheme. We have seen that constant-amplitude digital mod-

ulation schemes can give high-capacity systems. It should be pointed out that higher system-capacity levels can be expected if nonconstant-amplitude modulation schemes are acceptable.

A large number of unsolved problems remain. The analysis above (as indeed that in Refs. 1, 3, and 15) is based on very simple and idealized channel and interference models. More refined analysis and simulations will be necessary. The analysis above was carried out under the idealized assumptions of flat fading and of negligible effects of filtering and nonlinearities on the modulation scheme. Uniform transmission conditions were assumed for all cells. No delay spread was considered. Perfect timing and synchronization were assumed with coherent detection and ideal maximal-ratio combining. It was furthermore assumed that perfect synchronization for the time-division retransmission scheme was established. All of the above problems and others have to be taken into account in a refined system analysis.

At least the same number of channels seems to be within reach with the space-diversity and time-division retransmission schemes as with the spread spectrum multiple access approach to digital mobile radio (see Refs. 3, 19, 20, and 21).

## VI. ACKNOWLEDGMENT

Thanks are due to Tor Aulin, who calculated the fractional out-of-band power curves in Figs. 9 to 11 and to Arne Svensson, who calculated the error probability curves in Figs. 4 and 5 (see Ref. 12).

## REFERENCES

1. Y. S. Yeh and D. O. Reudink, "Efficient Spectrum Utilization for Mobile Radio Systems Using Space Diversity," *IEEE Trans. Commun.*, COM-30, No. 3 (March 1982), pp. 447-55.
2. V. H. MacDonald, "The Cellular Concept," *B.S.T.J.*, 58, No. 1 (January 1979), pp. 15-41.
3. P. S. Henry and B. S. Glance, "A New Approach to High Capacity Digital Mobile Radio," *B.S.T.J.*, 60, No. 8 (October 1981), pp. 1891-904.
4. W. C. Jakes, Jr., *Microwave Mobile Communications*, New York: Wiley, 1974.
5. T. Aulin and C.-E. Sundberg, "Continuous Phase Modulation—Part I: Full Response Signaling," *IEEE Trans. Commun.*, COM-29, No. 3 (March 1981), pp. 196-209.
6. T. Aulin, N. Rydbeck, and C.-E. Sundberg, "Continuous Phase Modulation—Part II: Partial Response Signaling," *IEEE Trans. Commun.*, COM-29, No. 3 (March 1981), pp. 210-25.
7. T. Aulin, C.-E. Sundberg, and A. Svensson, "MSK-Type Receivers for Partial Response Continuous Phase Modulation," *Int. Conf. Commun.*, Philadelphia, Pennsylvania, June 1982, pp. 6F3.1-6.
8. F. deJager and C. B. Dekker, "Tamed Frequency Modulation, A Novel Method to Achieve Spectrum Economy in Digital Transmission," *IEEE Trans. Commun.*, COM-26, No. 5 (May 1978), pp. 534-42.
9. R. deBuda, "Coherent Demodulation of Frequency-Shift Keying with Low Deviation Ratio," *IEEE Trans. Commun.*, COM-20 (June 1972), pp. 429-35.
10. K. Murota and K. Hirade, "GMSK Modulation for Digital Mobile Radio Telephony," *IEEE Trans. Commun.*, COM-29, No. 7 (July 1981), pp. 1044-50.
11. T. Aulin and C.-E. Sundberg, "Numerical Calculation of Spectra for Digital FM

- Signals," Nat. Telecommun. Conf., New Orleans, Louisiana, Conference Record, December 1981, pp. D.8.3.1-7.
12. C.-E. Sundberg, "Error Probability of Partial Response Continuous Phase Modulation With Coherent MSK-type Receiver Diversity and Slow Rayleigh Fading in Gaussian Noise," B.S.T.J., 61, No. 8 (October 1982), pp. 1933-63.
  13. T. Aulin, C.-E. Sundberg, and A. Svensson, "Viterbi Detectors with Reduced Complexity for Partial Response Continuous Phase Modulation," Nat. Telecommun. Conf., New Orleans, Louisiana, Conference Record, December 1981, pp. A.7.6.1-7.
  14. W. Hirt and S. Pasupathy, "Suboptimum Reception of Binary CPSK Signals," Proc. IEE, Part F, 128, No. 3 (June 1981), pp. 125-34.
  15. K. Murota, K. Konoshita, and K. Hirade, "Spectrum Efficiency of GMSK Land Mobile Radio," Int. Conf. Commun., Denver, Colorado, Conference Record, June 1981, pp. 23.8.1-5.
  16. C.-E. Sundberg, "Alternative Cell Configurations for Digital Mobile Radio Systems," B.S.T.J., this issue.
  17. M. Schwartz, W. R. Bennett, and S. Stein, *Communication Systems and Techniques*, New York: McGraw-Hill, 1966.
  18. D. Mulwijk, "Tamed Frequency Modulation—A Bandwidth-Saving Digital Modulation Method Suited for Land Mobile Radio," Philips Telecommun. Rev., 37, No. 1 (March 1979), pp. 35-49.
  19. G. R. Cooper and R. W. Nettleton, "A Spread-Spectrum Technique for High-Capacity Mobile Communications," IEEE Trans. Veh. Technol., VT-27 (November 1978), pp. 264-75.
  20. P. S. Henry, "Spectrum Efficiency of a Frequency-Hopped DPSK Spread-Spectrum Mobile Radio System," IEEE Trans. Veh. Technol., VT-28 (November 1979), pp. 327-32.
  21. D. J. Goodman, P. S. Henry, and V. K. Prabhu, "Frequency-Hopped Multilevel FSK for Mobile Radio," B.S.T.J., 59, No. 7 (September 1980), pp. 1257-75.

## APPENDIX

### *Details of adjacent-channel interference calculations*

In this appendix, we will demonstrate how the method for analyzing cochannel interference in Refs. 1 and 3, with minor modifications, can be used for calculation of adjacent-channel interference from adjacent (and further away) cells.

The average adjacent-channel interference from adjacent cells is calculated with basically the same method as the cochannel interference. It is assumed that the total adjacent-channel interference is formed by incoherent additions of several interference sources forming a stationary additive Gaussian noise, which is added to the cochannel interference noise. We will see that with "reasonable" spectral shape of the modulation scheme, this interference source is, in most cases, small compared to the cochannel interference.

Let  $A$  be the relationship between the adjacent-channel interference power on one side of the channel to the total power in this channel. This number is upper bounded by  $1/2$  of the fractional out-of-band power level at  $f = B_c$  (see Figs. 9 to 11 and Ref. 5). It is assumed that the receiver filter consists of an ideal bandpass filter of width  $B_c$  in these idealized calculations (the same assumptions are used in Ref. 15).

The base stations and the mobile units in nearby cells will cause adjacent-channel interference because of nonideal, nonband-limited

signals. We will consider the constant-amplitude raised cosine schemes (see Section II) transmitted without bandpass filtering. The spectral tails will cause adjacent-channel interference.

First, we will consider adjacent-channel interference for the case  $N = 3$ ,  $\alpha = 3$  with centrally located omnidirectional base stations (see Fig. 12). It is immediately clear from the frequency plan (Figs. 6a and 6b) that the adjacent-channel interference from sources within the same cell is extremely small with any spectrally efficient modulation scheme because each adjacent channel within one cell is three channels apart. The significant contributions to the total adjacent-channel interference come from adjacent channels in adjacent cells.

Once the major sources of interference are identified, it is straightforward to use the same methods as in Refs. 1, 3, and 16 for the calculation of the interference. The average adjacent-channel interference is suppressed by a factor of  $A$  compared to the cochannel inter-

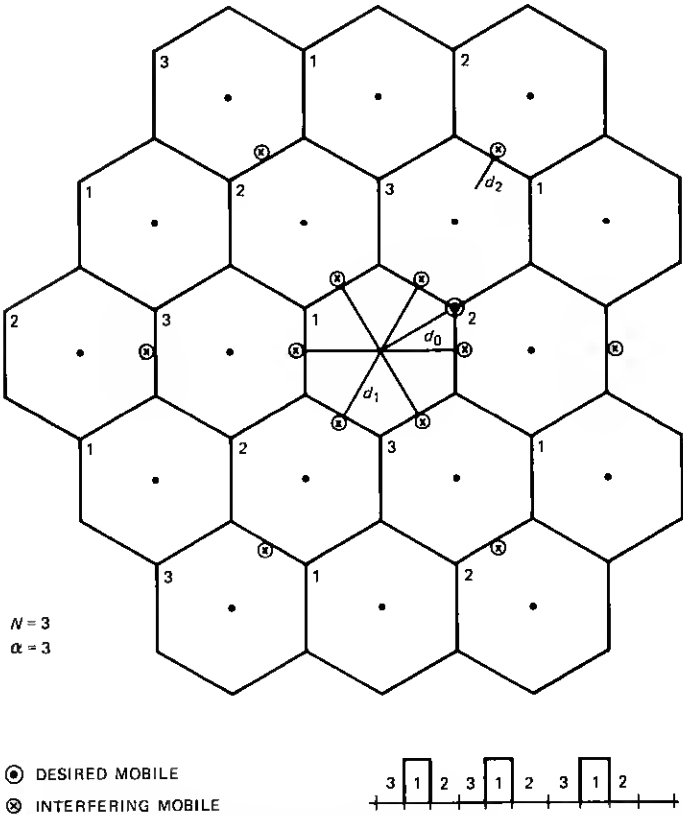


Fig. 12—Worst-case adjacent-channel interference cases for mobile-to-base transmission with centrally located antennas.

ference from the same sources. Space diversity helps against average adjacent-channel interference just as well as cochannel interference.<sup>1,3</sup>

Figure 12 shows the calculation of the worst-case (noncoherent addition) adjacent-channel interference for the  $N = 3$ ,  $\alpha = 3$  case with centrally located base stations and mobile-to-base transmission. Adjacent-channel interference comes from all cells marked 2 and 3. (Cochannel interference comes from cells marked 1; this is considered in Refs. 1, 3, and 16.) The distance to the desired mobile unit serviced from the omnidirectional antenna in the center of the cell is  $d_0$ . The distance to the nearest (worst-case) six interfering mobile units is  $d_1$  (see Fig. 12). The distance to the next six interfering mobile units is  $d_2$ . Thus, the worst-case adjacent-channel interference to signal ratio for mobile-to-base transmission is

$$\frac{P_I}{P_S} = A \left[ 6 \left( \frac{d_0}{d_1} \right)^3 + 6 \left( \frac{d_0}{d_2} \right)^3 + \text{further terms} \right]. \quad (16)$$

For the case in Fig. 12,

$$P_I/P_S \cong 9.5 \cdot A. \quad (17)$$

Assuming that the interfering mobile units can be in any equally probable location in their cells, we found that the average adjacent-channel interference to signal ratio for mobile-to-base is

$$P_I/P_S \cong 3.6 \cdot A. \quad (18)$$

It is straightforward to obtain similar results for base-to-mobile transmission for the case in Fig. 12. We have the adjacent-channel interference to signal ratio

$$P_I/P_S \cong 2.5 \cdot A. \quad (19)$$

It is also straightforward to calculate the formulas for a cell with three 120-degree corner stations in each cell (see Fig. 7). For  $N = 3$ ,  $\alpha = 3$ , we have for this case:

base-to-mobile,

$$P_I/P_S \cong 1.2A, \quad (20)$$

mobile-to-base average,

$$P_I/P_S \cong 1.5A. \quad (21)$$

In principle, it is straightforward to calculate the corresponding adjacent-channel interference formulas for the  $N = 3$ ,  $\alpha = 3$  case for other cells.<sup>16</sup> However, as a rough estimate one can use  $A$  times the cochannel-interference to signal ratio for the corresponding  $N = 1$  case.<sup>16</sup>

For all calculations above, it was assumed that the desired mobile unit is in the least favorable position in the cell, much the same way as in Refs. 1 and 16.

Note that in the approximate calculations above, we only considered averages. It is possible that the desired mobile unit and the interfering mobile unit in the adjacent cell occupying a frequency channel immediately adjacent to that of the desired mobile unit are almost at the same location near the cell dividing line. For such cases, the adjacent-channel interference might be such that the space diversity does not suppress this interference (the combiner in the desired mobile unit adds the interference and treats this interference just as the desired signal). For this case, a sufficiently small  $A$  is required. It is, of course, also conceivable to have a frequency channel change for one of the mobile units in that case.

For the  $N = 1$  case, the adjacent-channel interference problem becomes larger than for the  $N = 3$  case. The background average adjacent-channel interference from sources in adjacent cells is still there as before. On top of that, there is interference from (primarily two) adjacent channels within the cell of the desired mobile unit. A small  $A$  is required to suppress this interference.

#### AUTHOR

**Carl-Erik W. Sundberg**, M.S.E.E and Dr. Technology, Lund Institute of Technology, University of Lund, Lund, Sweden, in 1966 and 1975, respectively. Currently, Mr. Sundberg is a Research Professor in the Department of Telecommunication Theory, University of Lund. He is also Director of the consulting company SUNCOM, Lund. During 1976 he was with the European Space Research and Technology Centre (ESTEC), Noordwijk, The Netherlands, as an ESA Research Fellow. He has held positions as Consulting Scientist at LM Ericsson and SAAB-SCANIA, Sweden, and at Bell Laboratories, Crawford Hill, N. J. His research interests include source coding, channel coding, especially decoding techniques, digital modulation methods, fault-tolerant systems, digital mobile radio systems, spread spectrum systems, and digital satellite communication systems. He has published a large number of papers in these areas during the last couple of years. Dr. Sundberg holds several U.S. and European patents. Senior Member, IEEE; member, SER (Sveriges Elektroingenjörers Riksförening).

